ATR kinase is required for global genomic nucleotide excision repair exclusively during S phase in human cells

Yannick Auclair, Raphael Rouget, El Bachir Affar, and Elliot A. Drobetsky[1]

Maisonneuve-Rosemont Hospital Research Center, Faculty of Medicine, University of Montreal, Montréal, Québec, Canada

Edited by Richard B. Setlow, Brookhaven National Laboratory, Upton, NY, and approved September 25, 2008 (received for review February 19, 2008)

Global-genomic nucleotide excision repair (GG-NER) is the only pathway available to humans for removal, from the genome overall, of highly genotoxic helix-distorting DNA adducts generated by many environmental mutagens and certain chemotherapeutic agents, e.g., UV-induced 6–4 photoproducts (6–4PPs) and cyclobutane pyrimidine dimers (CPDs). The ataxia telangiectasia and rad-3-related kinase (ATR) is rapidly activated in response to UV-induced replication stress and proceeds to phosphorylate a plethora of downstream effectors that modulate primarily cell cycle checkpoints but also apoptosis and DNA repair. To investigate whether this critical kinase might participate in the regulation of GG-NER, we developed a novel flow cytometry-based DNA repair assay that allows precise evaluation of GG-NER kinetics as a function of cell cycle. Remarkably, inhibition of ATR signaling in primary human lung fibroblasts by treatment with caffeine, or with siRNA specifically targeting ATR, resulted in total inhibition of 6–4PP removal during S phase, whereas cells repaired normally during either G_0/G_1 or G_2/M. Similarly striking S-phase-specific defects in GG-NER of both 6–4PPs and CPDs were documented in ATR-deficient Seckel syndrome skin fibroblasts. Finally, among six diverse model human tumor strains investigated, three manifested complete abrogation of 6–4PP repair exclusively in S-phase populations. Our data reveal a highly novel role for ATR in the regulation of GG-NER uniquely during S phase of the cell cycle, and indicate that many human cancers may be characterized by a defect in this regulation.

cell cycle | flow cytometry | nucleotide excision repair | UV-induced DNA photoproducts

Nucleotide excision repair (NER) forestalls neoplastic transformation by removing an array of helix-distorting, replication-blocking DNA adducts generated by a multitude of environmental carcinogens, as well as by certain widely used chemotherapeutic drugs. These so-called "bulky DNA lesions" include ultraviolet (UV)-induced cyclobutane pyrimidine dimers (CPDs) and 6–4 photoproducts (6–4PPs), which play key roles in the pathogenesis of sunlight-induced skin cancer (1) and constitute ideal model DNA lesions for dissecting the mechanism of NER. The clinical relevance of NER is highlighted by patients afflicted with *Xeroderma pigmentosum* who carry inactivating mutations in specific NER pathway genes, are defective in the removal of bulky DNA adducts, and display striking predisposition to cutaneous tumor development (2).

NER is comprised of two overlapping subpathways. Global genomic NER (GG-NER) removes DNA damage from anywhere within the nuclear genome, and is initiated when the UV-DDB1/UV-DDB2 and then XPC/HR23B heterodimers recognize the helical distortion introduced into DNA by bulky adducts and bind to the damaged site (3). The "core NER pathway" is then recruited and removes the lesion through sequential steps of strand unwinding, incision in a number of bases on either side of the lesion, excision of the lesion as part of a short single-stranded oligonucleotide, and filling in of the resultant gap using semiconservative DNA replication factors and the nondamaged complementary strand as template. The other NER subpathway, transcription-coupled NER, removes bulky DNA adducts exclusively from the transcribed strand of active genes (4). This subpathway differs from GG-NER only in the manner of lesion recognition, i.e., it is triggered by blockage of RNA polymerase II at adducted sites along the transcribed strand. This is followed by binding of the CS-A and CS-B proteins and recruitment of the core NER pathway, which then, in the identical manner as GG-NER, completely restores the integrity of the DNA.

After treatment with the model mutagen 254-nm UV (hereafter designated UV) or other replication stress-inducing agents, the ataxia-telangiectasia and rad3-related kinase (ATR) is rapidly activated (5), and in turn phosphorylates the p53 tumor suppressor thereby contributing to the latter's stabilization and function (6). In addition, previous reports have demonstrated that for most UV-exposed cell types, p53 is required for efficient repair of CPDs via GG-NER (7, 8). However the situation for 6–4PPs remains less clear with various studies showing that loss of p53 reduces (9–11) or has no influence (12, 13) on removal of this photoproduct. In any case it is conceivable *a priori* that ATR regulates p53-dependent GG-NER; moreover this kinase may also be expected to participate in GG-NER independently of p53. Indeed, during replication stress, ATR phosphorylates a multitude of substrates aside from p53 that modulate primarily cell cycle checkpoints but also apoptosis and DNA repair, including various proteins implicated in GG-NER (see Discussion). Despite this, no previous studies to our knowledge have thoroughly directly evaluated GG-NER kinetics in cultured human cells after abrogation of ATR signaling.

Here we explore the possibility that ATR regulates GG-NER, possibly in an S-phase-specific manner given the preeminent role of this kinase in safeguarding semiconservative DNA replication during genotoxic stress. In a novel approach, a flow cytometry-based assay recently developed (14) was optimized to precisely evaluate the kinetics of UV DNA photoproduct repair as a function of cell cycle. We were able to conclusively demonstrate that during S, but not G_0/G_1 or G_2/M, removal of UV-induced DNA damage via GG-NER in human cells is strictly dependent upon ATR, revealing a highly novel function for this kinase in the maintenance of genomic stability. Moreover we show that among six model human tumor strains investigated, three exhibit complete deficiency in GG-NER exclusively during S phase, implying

Author contributions: Y.A., R.R., and E.B.A. performed research; Y.A., R.R., and E.B.A. contributed new reagents/analytic tools; Y.A. and E.D. analyzed data; Y.A. and E.D. designed research; and Y.A. and E.D. wrote the paper.

The authors declare no conflict of interest.

This article is a PNAS Direct Submission.

[1]To whom correspondence should be addressed. E-mail: elliot.drobetsky@umontreal.ca.

This article contains supporting information online at www.pnas.org/cgi/content/full/0801585105/DCSupplemental.

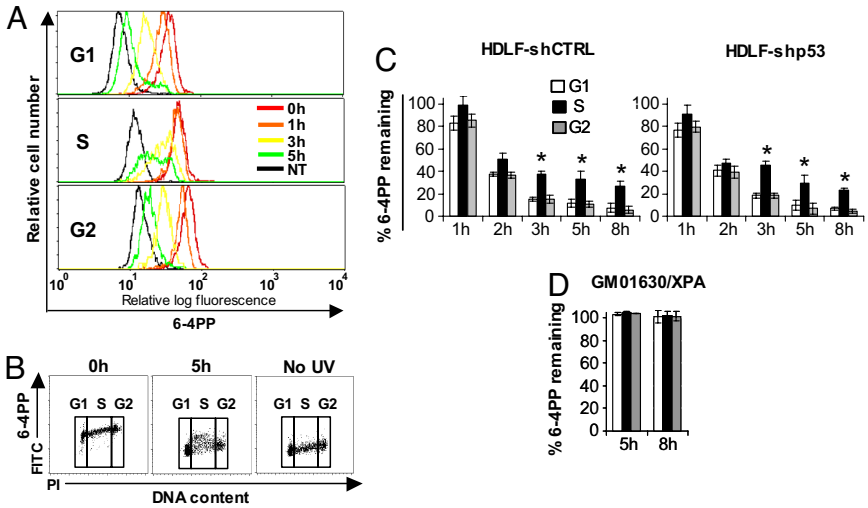

Fig. 1. GG-NER of 6–4PPs in individual phases of the cell cycle in HDLFs. (*A*) Representative histogram overlay illustrating repair of 6–4PPs in each phase of the cell cycle in HDLF-shCTRL. (*B*) Bivariate distributions of 6–4PP (FITC; log scale) versus DNA content (PI; linear scale) in HDLF-shCTRL. (*C*) Graphical depictions of 6–4PP removal in HDLFs differing in p53 status and (*D*), in XPA-deficient HDSFs. Mean ± SEM from three independent experiments is shown. *, $P < 0.05$; two-tailed paired *t* test (S phase relative to G_1).

that a similar cell-cycle-specific repair defect may be present in many human cancers.

Results

Optimization of a Flow-Cytometry-Based Assay to Quantify DNA Photoproduct Removal in Individual Phases of the Cell Cycle. We recently reported on the development of a flow cytometry-based fluorescence assay permitting evaluation of GG-NER kinetics in UV-exposed cells stained with anti-CPD or anti-6–4PP antibodies (14). During the course of this investigation, before UV exposure, cellular proliferation was abolished by growth to confluence or serum starvation (synchronization in G_0/G_1). Such an approach has traditionally been taken to ensure accurate determination of GG-NER kinetics, which requires that newly replicated (nondamaged) DNA generated during post-UV incubations be either rigorously controlled for or excluded from consideration. In fact, a considerable majority of previous studies using various direct assays for monitoring UV DNA photoproduct removal was performed under conditions in which S-phase DNA had been eliminated from the analysis.

In the present case, we were interested in evaluating whether GG-NER might be regulated by ATR as a function of cell cycle, and thus proceeded to optimize our assay such that DNA photoproduct removal could be precisely monitored in each of G_0/G_1, S, and G_2/M. For this initial purpose we chose as experimental model isogenic primary human lung fibroblast (HDLF) strains stably expressing either an shRNA targeting p53 (HDLF-shp53) or a scrambled shRNA sequence (HDLF-shCTRL). As expected, p53 was strongly expressed in HDLF-shCTRL at 6 h post-UV, but only barely detectable in the shp53-expressing counterpart [supporting information (SI) Fig. S1*A*].

As a critical control, HDLF-shCTRL cells were first irradiated with 25 J/m^2 or mock irradiated, followed immediately by incubation with the mitotic inhibitor nocodazole to block reentry of cells from G_2/M to G_0/G_1. Flow-cytometric analysis of propidium iodide (PI)-stained cells (15) then revealed, as fully expected, that most of the nocodazole-treated, mock-irradiated HDLF-shCTRL cells had accumulated in G_2/M at 24 h (Fig. S1*B*). However, consistent with the well-characterized ability of UV to induce transient growth arrest throughout the cell cycle, no significant progression was observed within 24 h post-UV. Very similar results were obtained for HDLF-shp53 treated with nocodazole with or without UV (data not shown). We thus concluded that for HDLFs irradiated with 25 J/m^2 UV, GG-NER kinetics could be accurately measured in individual phases of the cell cycle within the first 24 h without any need to control for cellular proliferation. This permitted us to use our flow cytometry-based repair assay precisely as described (14), except that in the present circumstance exponentially growing, asynchronous (rather than G_0/G_1-synchronized) cells were UV irradiated followed by determination of repair kinetics for populations gated in each of G_0/G_1, S, and G2/M.

Here we have focused primarily on 6–4PPs, which are repaired via GG-NER much more rapidly than CPDs, i.e., generally 80–100% removal within 6–8 h post-UV for 6–4PPs, and 30–60% removal at 24 h post-UV for CPDs (16). A representative histogram overlay, depicting the kinetics of 6–4PP repair in each of G_0/G_1, S, or G_2/M for UV-exposed HDLF-shCTRL cells, is shown (Fig. 1*A*). In each phase, most markedly S, the increased width of peaks with time indicates heterogeneity for repair within the population, a phenomenon that is visually apparent in the representative dot plot (Fig. 1*B*). As shown in Fig. 1*C*, on average 80–95% of 6–4PPs are removed in HDLF-shCTRL by 3–5 h post-UV during G_0/G_1 or G_2/M, whereas repair efficiency is moderately but significantly diminished during S (60–75% removal). Of note, HDLF-shp53 exhibited very similar kinetics of 6–4PP removal relative to HDLF-shCTRL, strongly supporting the notion that p53 generally is not required for GG-NER of this photoproduct in human cells. As negative control, NER-deficient primary skin fibroblasts, derived from an XPA patient, were confirmed to be completely defective in 6–4PP repair during all phases of the cell cycle (Fig. 1*D*).

Abrogation of Signaling Through ATR, but Not Through ATM, Completely Abolishes 6–4PP Repair Exclusively During S Phase. To initially evaluate whether ATR might regulate GG-NER, HDLFs were pretreated with 10 mmol/l caffeine, which strongly inhibits ATR signaling (17). We demonstrated by immunofluorescence microscopy that, in the manner expected (18), caffeine treatment abrogated ATR-mediated phosphorylation of H2AX after UV (Fig. S2*A*). As depicted in the representative profiles and accompanying histogram (Fig. 2 *A* and *B*), strikingly, 10 mmol/l caffeine completely abolished 6–4PP repair during S, whereas

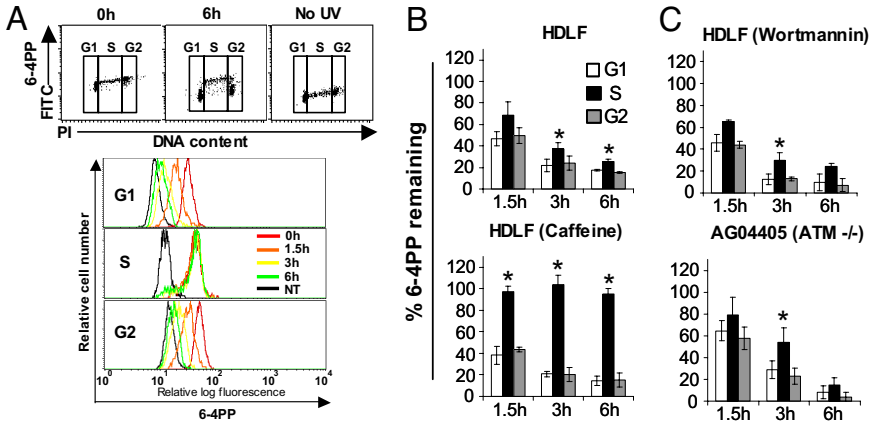

Fig. 2. Pharmacological abrogation of signaling through ATR but not through ATM completely abolishes GG-NER of 6–4PPs in HDLFs during S but not during G_0/G_1 or G_2/M. (*A*) Representative results depicting cell cycle-specific 6–4PP repair in HDLFs treated with 10 mmol/l of caffeine; (top panel) Bivariate distributions of 6–4PP (FITC) versus DNA content (PI); (bottom panel) representative histogram overlay illustrating repair of 6–4PP. (*B*) Graphical depiction of 6–4PP repair in wild-type HDLFs treated or not with 10 mmol/l caffeine followed by irradiation with UV. (*C*) Graphical depictions of 6–4PP repair in wild-type HDLFs treated with 30 μmol/l wortmannin, and in the ATM-deficient cell line AG04405A, following irradiation with UV. Mean ± SEM from three independent experiments is shown. *, $P < 0.05$; two-tailed paired *t* test (S phase relative to G_1).

repair was efficient during G_0/G_1 or G_2/M. Because the efficiency of UV DNA photoproduct repair can vary significantly as a function of dose (19), we also investigated 6–4PP repair in HDLFs with or without caffeine after irradiation with 10 J/m^2. At this dose, repair efficiency was consistently lower during S relative to the other phases (Fig. S3*A*) although unlike for 25 J/m^2 this reduction was not statistically significant. Importantly however, in accordance with the findings for 25 J/m^2, caffeine treatment profoundly abrogated GG-NER of 6–4PPs exclusively during S phase in HDLFs irradiated with 10 J/m^2 (Fig. S3*B*).

Although the above data suggest that ATR might regulate GG-NER uniquely during S phase, the participation of other PI3 kinases known to be caffeine sensitive cannot be ruled out. In particular, the ataxia telangiectasia-mutated kinase (ATM) is strongly inhibited by 10 mmol/l caffeine; moreover ATM was recently shown to be phosphorylated after UV and has previously been implicated in NER (see Discussion). HDLFs were thus cultured in the presence of 30 μmol/l wortmannin, which inhibits signaling through ATM but not ATR (20). Moreover this treatment, as expected (21), abrogated phosphorylation of H2AX after exposure to IR but not UV (Fig. S2*A*,*B*). We found that these wortmannin-treated HDLFs, as well as primary skin fibroblasts derived from an ATM-deficient patient, carried out relatively efficient repair of 6–4PPs in all phases of the cell cycle (Fig. 2*C*).

To unequivocally confirm a role for ATR in S-phase-specific GG-NER, HDLFs were transiently transfected with an siRNA pool targeting this kinase, which resulted in ≈90% reduction of ATR protein levels as measured by densitometry (Fig. 3*A*, top panel). Moreover immunofluorescence microscopy demonstrated that ATR-dependent phosphorylation of H2AX was abrogated after UV in siATR-treated HDLFs relative to controls expressing scrambled siRNAs (Fig. 3*A*, bottom panel). Remarkably, in accord with our results in caffeine-treated cells, Fig. 3B clearly depicts complete abolition of 6–4PP removal in siATR-HDLFs during S phase, whereas repair during G_0/G_1 or G_2/M is not affected. On the other hand, repair rates appeared normal in all phases in control HDLFs. The above data, taken together, conclusively demonstrate the existence of a highly novel ATR-dependent regulation of GG-NER operating exclusively during S phase in human cells.

ATR-Deficient Seckel Syndrome Skin Fibroblasts Are Profoundly Defective in S-Phase-Specific GG-NER of 6–4PPs and CPDs. We next analyzed the kinetics of 6–4PP removal in the ATR-deficient Seckel syndrome skin fibroblast strain F02–98 following UV. Relative to the closely related wild-type counterpart 1BR, F02–98 exhibited profoundly reduced levels of ATR protein expression, and of H2AX phosphorylation after UV (Fig. 4*A*). Furthermore, as for HDLFs, cell cycle progression in 1BR and F02–98 was abolished for at least 24 h post UV (data not shown). Consistent with the striking results in Figs. 2 and 3, F02–98 exhibited complete abrogation of 6–4PP removal uniquely during S whereas 1BR repaired normally (Fig. 4B). GG-NER of CPDs was also evaluated in the above paired strains. At 12 and 24 h post-UV ≈15% and 25% of CPDs, respectively, were removed with similar efficiency in all phases of the cell cycle in 1BR. (In contrast with the situation for 6–4PPs in HDLFs, no apparent slowdown of CPD repair during S phase was noted in

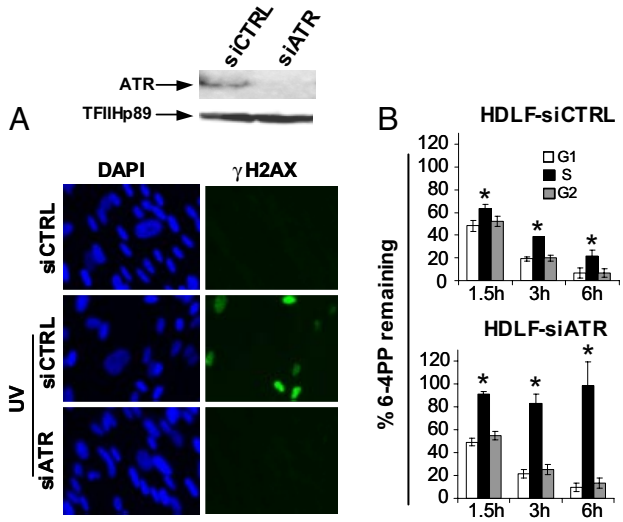

Fig. 3. ATR is strictly required for GG-NER of 6–4PPs exclusively during S phase of the cell cycle in HDLFs. (*A*) Western blot showing expression of ATR (top panel), and immunostaining of γH2AX (bottom panel), 2 hours after irradiation with UV in HDLFs transfected with control siRNAs versus siRNAs targeting ATR. (*B*) Graphical depictions of 6–4PP repair in HDLFs transfected with control siRNAs or with siRNAs targeting ATR and irradiated with UV. Mean ± SEM from three independent experiments is shown. *, $P < 0.05$; two-tailed paired *t* test (S phase relative to G_1).

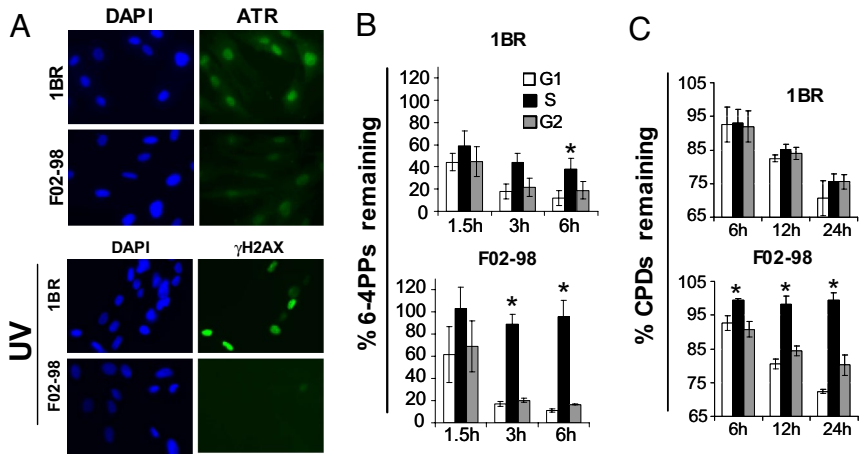

Fig. 4. Removal of UV-induced DNA photoproducts is abrogated uniquely during S phase in ATR-deficient Seckel syndrome skin fibroblasts. (*A*) Immunostaining of ATR protein (top panel) and of γH2AX (bottom panel) 2 hours post-UV in Seckel syndrome F02–98 skin fibroblasts versus the closely related normal counterpart 1BR. (*B*) Graphical depiction of 6–4PP repair and (*C*) of CPD repair, in F02–98 versus 1BR. Mean ± SEM from three independent experiments is shown. *, $P < 0.05$; two-tailed paired *t* test (S phase relative to G_1).

1BR.) On the other hand, although F02–98 manifested similar CPD removal rates during G_0/G_1 and G_2/M, repair was totally abolished during S at all time points (Fig. 4C). These data indicate that removal of CPDs, as well as of 6–4PPs, is strictly regulated in an ATR-dependent manner uniquely during S phase.

GG-NER of 6–4PPs Is Abolished During S Phase in Diverse Model Tumor Cell Lines. Having evaluated cell cycle specificity for GG-NER of 6–4PPs in various human fibroblast strains differing in p53, ATR, or ATM status, we turned our attention to cancer cells. Repair of 6–4PP was investigated in six model tumourigenic strains, i.e., U2OS osteosarcoma, 293 embryonic kidney, DLD-1 colorectal carcinoma, SAOS-2 osteosarcoma, A549 lung carcinoma, and MCF-7 breast carcinoma. Primary human skin fibroblasts (HDSFs) were also investigated as control. For each of the tumor strains, flow-cytometric analysis of PI-stained cells showed that cell cycle progression was abolished within the first 6 h post-UV after exposure to 25 J/m^2 (data not shown). For HDSFs, in accord with the situation for HDLFs, up to 75% and 95% of 6–4PP were removed by 3 h and 6 h post-UV, respectively, in G_0/G_1 or G_2/M, whereas during S these values were significantly reduced, i.e., were only 40% and 75% (Fig. 5). The combined data in primary HDSFs and HDLFs suggest that nonimmortalized strains can exhibit modest but significant reductions in the efficiency of 6–4PP removal during S relative to G_0/G_1 or G_2/M under normal culture conditions. Strikingly, however, three tumor strains, i.e., A549, MCF-7, and U2OS, exhibited complete abrogation of 6–4PP repair exclusively during S (Fig. 5). On the other hand, in the case of DLD-1, SAOS-2, and 293, 6–4PP removal was rapid and equivalent during all phases. Of note, the three tumor strains deficient in 6–4PP removal during S express ATR protein and are proficient in phosphorylation of H2AX after UV (Fig. S4). Moreover these latter three strains are all known to be p53-proficient, whereas those exhibiting no differences in repair among the cell cycle phases have been characterized as p53 deficient.

Discussion

Here we report on the development and use of a novel flow-cytometry-based assay that allows precise determination of GG-NER kinetics as a function of cell cycle. In initially investigating UV-irradiated cells under normal culture conditions, we showed that removal of 6–4PPs in HDLFs or HDSFs irradiated with 25 J/m^2 UV was moderately but significantly slower during S relative to G_0/G_1 or G_2/M. This S-phase-specific reduction in GG-NER efficiency in primary fibroblasts may not be actively regulated, but rather could reflect, for example, differences among the cell cycle phases with respect to chromatin structure or other determinants affecting access of repair proteins to sites of DNA damage. In any case, unlike the situation for primary lung or skin fibroblasts, we observed equivalent repair kinetics during all phases of the cycle for (*i*) 6–4PPs in three model tumor cell lines, (*ii*) 6–4PPs in HDLFs treated with 10J/m^2 UV, and (*iii*)

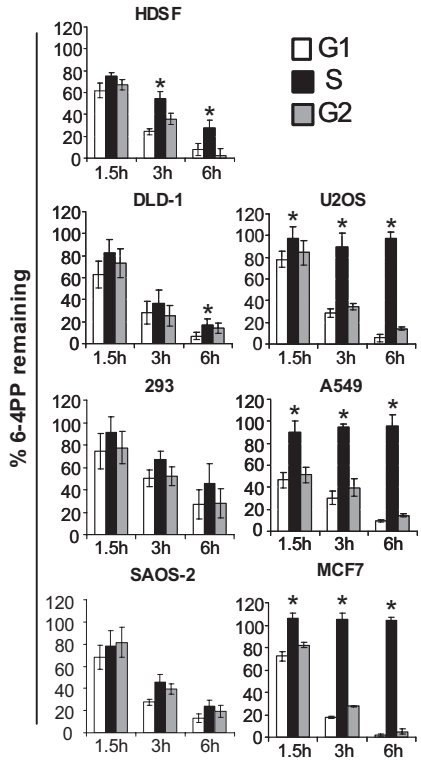

Fig. 5. Cell cycle-specific repair of UV DNA photoproducts in human tumor cell lines. Graphical depictions of 6–4PP repair in HDSFs and in various tumor strains irradiated with 25 J/m^2 of UV. Mean ± SEM of three independent experiments is shown. *, $P < 0.05$; two-tailed paired *t* test (S relative to G_1).

for CPDs in hTERT-immortalized 1BR skin fibroblasts. It should also be emphasized that a few prior studies have evaluated GG-NER rates as a function of cell cycle under normal culture conditions. Of particular relevance here, in contrast with our results, using a well-established RIA it was shown in primary skin fibroblasts (22) or primary lymphoblasts (23) that removal of 6–4PP is not influenced by cell cycle. Other studies also performed in primary fibroblasts or lymphoblasts indicated that GG-NER rates may actually be relatively faster during S or G_0/G_1, respectively (24, 25). It must be emphasized that the above investigations each used different GG-NER assays and different methods for isolating cell populations in specific phases. The overall data thus indicate that cell-cycle-specific variations in GG-NER efficiency under normal culture conditions might reflect the repair assay, dose, and/or particular DNA adduct studied. We suggest that future investigations using diverse primary and cancer cell types in conjunction with the powerful flow-cytometry-based repair assay described herein could eventually establish a firm consensus regarding this issue.

Having established a method for evaluating GG-NER kinetics as a function of cell cycle, we proceeded to conclusively demonstrate that ATR is strictly required for GG-NER exclusively during S, thereby revealing a highly novel role for this kinase in the maintenance of genomic stability. In addition, our data strongly indicate that ATM is not involved in S-phase-specific regulation of repair. We believe it important to address the potential role of ATM, as this kinase, once widely considered not to be capable of being activated by UV, can in fact become phosphorylated following UV in an ATR-dependent manner (26). Moreover ATM had been shown (*i*) to physically interact with components of the NER machinery after treatment with the UV-mimetic agent cisplatin (27), and (*ii*) to phosphorylate the NER pathway factor RP-A (replication protein-A) in response to UV (28).

The precise ATR substrate(s) that regulate S-phase-specific GG-NER remain(s) to be identified. Our data on 6–4PP repair in HDLFs expressing shRNA targeting p53 (Fig. 1), and in p53-deficient vs. p53-proficient tumor cell strains (Fig. 5), taken together strongly indicate that p53 does not participate in this regulation. However, in response to UV, ATR rapidly phosphorylates a plethora of proteins aside from p53 that regulate primarily cell cycle checkpoints but also apoptosis and DNA repair. Regarding potential ATR substrates that may regulate S-phase-specific repair independently of p53, it is noteworthy that RP-A is phosphorylated on multiple serine/threonine residues by ATR post-UV (29) and plays a central role not only in semiconservative DNA replication but also in both the lesion recognition- and gap filling-steps of GG-NER (30). We also highlight an extensive proteomics analysis recently identifying XPC and XPA as potential ATR substrates during genotoxic stress (31). Furthermore firm experimental evidence was presented showing that XPA is indeed phosphorylated by ATR on serine 196 after UV, and that this event is required for maintaining UV resistance (32). A follow-up investigation demonstrated that redistribution of XPA to the nucleus is also dependent on ATR but, interestingly, not on serine 196 phosphorylation (33).

In addition to the above ATR substrates participating directly in GG-NER, others have been firmly implicated in this pathway. The BRCA1 tumor suppressor is phosphorylated by ATR on multiple serine residues in response to UV (34), and moreover has previously been implicated in p53-independent regulation of GG-NER (35). In addition, the recently identified replication-checkpoint protein claspin is phosphorylated in an ATR-dependent manner after UV (36) and was shown to interact directly with UV-DDB1, UV-DDB2, and XP-C (37). Although this latter study demonstrated that RNAi-mediated knockdown of claspin does not affect GG-NER, repair was not monitored specifically in S-phase cells. In conclusion, it remains to be evaluated whether loss of ATR-dependent phosphorylation of any among RPA, XPA, XPC, BRCA1, or claspin might abrogate GG-NER in UV-exposed cells during S phase, but not during G_0/G_1 or G_2/M.

The intriguing observation here that three among six randomly chosen model human tumor cell lines are totally deficient in GG-NER exclusively during S implies that many human cancers may be characterized by such a defect. However any potential link between ATR signaling and the striking repair defect in these model tumor strains remains to be determined. Because all three strains express ATR protein and are proficient in H2AX phosphorylation, we offer reasonable speculation that they are nonetheless defective in ATR-mediated phosphorylation of particular downstream effectors which regulate S-phase-specific GG-NER. Thus our data in tumor cell lines may relate to a heretofore unidentified, critical underlying factor in the development of multistage carcinogenesis, where exposure to bulky adduct-inducing environmental genotoxins and subsequent mutation fixation in critical growth control genes plays an important role. Moreover our findings potentially harbor important implications for cancer treatment. Indeed burgeoning evidence supports the notion that NER status of tumors is a major determinant in the clinical response to cisplatin (38), which, like UV, exerts powerful cytotoxic effects via the induction of bulky DNA adducts (39). As such, human cancers that might be identified as totally deficient in S-phase-specific GG-NER would be expected to respond much more effectively, and possibly more selectively, to treatment protocols that include UV-mimetic chemotherapeutic drugs.

Materials and Methods

Cell Culture. Primary lung fibroblasts (HDLFs) were kindly provided by Dr. J. Sedivy (Brown University). The hTERT-immortalized Seckel syndrome skin fibroblast strain F02–98 (carrying a hypomorphic ATR splice-site mutation that profoundly reduces ATR protein expression) (40) and the closely related wild-type hTERT-immortalized control strain 1BR, were a gift of Dr. P. Jeggo (University of Sussex). Normal primary skin fibroblasts (HDSFs; GM01652B), XPA-deficient HDSFs (GM01630), and ATM-deficient HDSFs (AG04405A) were purchased from the Coriell Institute. The above strains were cultured in Eagle's MEM supplemented with 15% fetal bovine serum, L-glutamine, and antibiotics (Wisent, Montreal, Canada). Model tumor strains (U2OS, SAOS-2, 293, DLD-1, A549, and MCF7) were grown in Dulbecco's MEM supplemented with 10% fetal bovine serum, L-glutamine, and antibiotics.

Attenuation of p53 and ATR Expression in HDLFs. For pharmacological inhibition of ATR and ATM, or ATM but not ATR, 10 mmol/l caffeine (Sigma) or 30 μmol/l wortmannin (Calbiochem), respectively, were added to cultures 30 minutes before UV treatment. Knockdown of p53 expression in HDLFs by stable expression of shRNA targeting p53, driven by the pSUPER retroviral vector, was performed as described (14). For siRNA-mediated knockdown of ATR, 2×10^5 cells were plated in 35-mm dishes 1 day before siRNA transfection in complete growth media without antibiotics. siRNAs targeting human ATR (sc-29763), or nontargeting siRNAs (sc-37007), were purchased from Santa Cruz. siRNAs were transfected into cells using Lipofectamine 2000 according to the manufacturer's (Invitrogen) directions, and cells were used at 2 days posttransfection.

Irradiation Conditions. Cell monolayers growing in 60-mm dishes were washed thoroughly with phosphate-buffered saline (PBS) and covered with 2 ml of PBS, followed by UV irradiation with a Philips G25T8 germicidal lamp at a fluence of 0.2 J/m^2/s.

Protein Detection. Western blotting using antibodies (Santa Cruz) for p53 (DO-1 antibody; 1:5000 dilution), ATR (N-19 antibody, 1:500 dilution), and TFIIHp89 (S-19 antibody, 1:500 dilution) was performed as previously described (15).

For immunofluorescence detection of γ-H2AX or ATR, cells were grown on coverslips in 35-mm dishes, treated with UV, and fixed for 15 minutes in PBS/3% paraformaldehyde. Cells were then washed with PBS and permeabilized for 10 minutes in PBS/0.5% Triton X-100, blocked for 1 h in PBS/10%

FBS/0.1% Triton X-100, and incubated with a primary mouse monoclonal anti-human γ-H2AX antibody (1:500; Upstate) or goat polyclonal anti-human ATR antibody (N-19 antibody, 1:50, Santa Cruz Biotechnology) for 2 hours. Cells were washed with PBS and incubated for 1 h with an Alexa 488 goat anti-mouse IgG secondary antibody or an Alexa 488 donkey anti-goat IgG secondary antibody (Molecular Probes). Cells were washed with PBS and nuclei stained with 0.2 μg/ml DAPI (Sigma). Fluorescence was visualized with a Leica DMRE microscope, and data acquired using a RETIGA EX digital camera (QIMAGING) coupled with OpenLab 3.1.1 software (OpenLab).

Determination of GG-NER Kinetics as a Function of Cell Cycle. Exponentially growing, asynchronous monolayers were UV-irradiated and immediately refed with normal culture medium. At various times posttreatment, cultures were washed with PBS, trypsinized, resuspended in 1 ml of PBS, and fixed by addition of 3 ml ice-cold 100% ethanol. Next, 2.5×10^5 fixed cells were resuspended in either 0.5% Triton-X-100/2 N HCl (for CPD detection) or 0.5% Triton-X-100/0.2 N HCl (for 6–4PP detection), and incubated for 10 minutes at 22 °C. Cells were washed with 0.1 mol/l $Na_2B_4O_7$ (pH 9.0) and then with PBS, and resuspended in 300 μl of RNase (100 μg/ml in PBS) for 1 h at 37 °C. Cells were centrifuged and resuspended in 300 μl PBS-TB (1% BSA/0.25% Tween-20/PBS) containing a primary monoclonal antibody (1:1000; Kamiya Biomedical) against either CPDs or 6–4 PPs for 1.5 h at 22 °C, followed by washing with PBS-TB and resuspension in 300 μl of PBS-TB containing FITC-conjugated rabbit anti-mouse secondary antibody (1:200) for 1 h at 22 °C. Pellets were then washed twice with PBS-TB and resuspended in 300 μl PBS containing 5 μg/ml PI (Molecular Probes). Cells were gated in each phase of the cell cycle and repair kinetics monitored using a flow cytometer (fitted with an argon laser and CellQuestPro software; Becton Dickinson) to quantify the change in geometric mean fluorescence over time, with correction for background autofluorescence.

ACKNOWLEDGMENTS. This work was supported by a grant from the Canadian Institutes for Health Research (to E.A.D.).

1. Melnikova VO, Ananthaswamy HN (2005) Cellular and molecular events leading to the development of skin cancer. *Mutat Res* 571:91–106.
2. Kraemer KH, Lee MM, Scotto J (1984) DNA repair protects against cutaneous and internal neoplasia: Evidence from xeroderma pigmentosum. *Carcinogenesis* 5:511–514.
3. Gillet LC, Scharer OD (2006) Molecular mechanisms of mammalian global genome nucleotide excision repair. *Chem Rev* 106:253–276.
4. Fousteri M, Mullenders LH (2008) Transcription-coupled nucleotide excision repair in mammalian cells: Molecular mechanisms and biological effects. *Cell Res* 18:73–84.
5. Paulsen RD, Cimprich KA (2007) The ATR pathway: Fine-tuning the fork. *DNA Repair* 6:953–966.
6. Tibbetts RS *et al.* (1999) A role for ATR in the DNA damage-induced phosphorylation of p53. *Genes Dev* 13:152–157.
7. Ford JM, Hanawalt PC (1995) Li-Fraumeni syndrome fibroblasts homozygous for p53 mutations are deficient in global DNA repair but exhibit normal transcription-coupled repair and enhanced UV resistance. *Proc Natl Acad Sci* 92:8876–8880.
8. Mathonnet G *et al.* (2003) UV wavelength-dependent regulation of transcription-coupled nucleotide excision repair in p53-deficient human cells. *Proc Natl Acad Sci* 100:7219–7224.
9. Tron VA *et al.* (1998) p53-dependent regulation of nucleotide excision repair in murine epidermis in vivo. *J Cutan Med Surg* 3:16–20.
10. Ford JM, Hanawalt PC (1997) Expression of wild-type p53 is required for efficient global genomic nucleotide excision repair in UV-irradiated human fibroblasts. *J Biol Chem* 272:28073–28080.
11. Ford JM, Baron EL, Hanawalt PC (1998) Human fibroblasts expressing the human papillomavirus E6 gene are deficient in global genomic nucleotide excision repair and sensitive to ultraviolet irradiation. *Cancer Res* 58:599–603.
12. Adimoolam S, Lin CX, Ford JM (2001) The p53-regulated cyclin-dependent kinase inhibitor, p21 (cip1, waf1, sdi1), is not required for global genomic and transcription-coupled nucleotide excision repair of UV-induced DNA photoproducts. *J Biol Chem* 276:25813–25822.
13. Ferguson BE, Oh DH (2005) Proficient global nucleotide excision repair in human keratinocytes but not in fibroblasts deficient in p53. *Cancer Res* 65:8723–8729.
14. Rouget R *et al.* (2007) A sensitive flow cytometry-based nucleotide excision repair assay unexpectedly reveals that mitogen-activated protein kinase signalling does not regulate the removal of UV-induced DNA damage in human cells. *J Biol Chem* 283:5533–5541.
15. Loignon M, Drobetsky EA (2002) The initiation of UV-induced G(1) arrest in human cells is independent of the p53/p21/pRb pathway but can be attenuated through expression of the HPV E7 oncoprotein. *Carcinogenesis* 23:35–45.
16. Mitchell DL, Haipek CA, Clarkson JM (1985) (6–4) Photoproducts are removed from the DNA of UV-irradiated mammalian cells more efficiently than cyclobutane pyrimidine dimers. *Mutat Res*, 143:109–112.
17. Sarkaria JN *et al.* (1999) Inhibition of ATM and ATR kinase activities by the radiosensitizing agent, caffeine. *Cancer Res* 59:4375–4382.
18. Hanasoge S, Ljungman M (2007) H2AX phosphorylation after UV irradiation is triggered by DNA repair intermediates and is mediated by the ATR kinase. *Carcinogenesis* 28:2298–2304.
19. Greinert R, *et al.* (2000) The dose dependence of cyclobutane dimer induction and repair in UVB-irradiated human keratinocytes. *Photochem Photobiol* 72:701–708.
20. Sarkaria JN *et al.* (1998) Inhibition of phosphoinositide 3-kinase related kinases by the radiosensitizing agent wortmannin. *Cancer Res* 58:4375–4382.
21. Burma S *et al.* (2001) ATM phosphorylates histone H2AX in response to DNA double-strand breaks. *J Biol Chem*, 276:42462–424567.
22. Wang YC, Maher VM, Mitchell DL, McCormick JJ (1993) Evidence from mutation spectra that the UV hypermutability of xeroderma pigmentosum variant cells reflects abnormal, error-prone replication on a template containing photoproducts. *Mol Cell Biol* 13:4276–4283.
23. Mitchell DL, Cleaver JE, Lowery MP, Hewitt RR (1995) Induction and repair of (6–4) photoproducts in normal human and xeroderma pigmentosum variant cells during the cell cycle. *Mutat Res* 337:161–167.
24. Tommasi S, Oxyzoglou AB, Pfeifer GP (2000) Cell cycle-independent removal of UV-induced pyrimidine dimers from the promoter and the transcription initiation domain of the human CDC2 gene. *Nucleic Acids Res* 28:3991–3998.
25. Thyagarajan B *et al.* (2007) Alkaline unwinding flow cytometry assay to measure nucleotide excision repair. *Mutagenesis* 22:147–153.
26. Stiff T *et al.* (2006) ATR-dependent phosphorylation and activation of ATM in response to UV treatment or replication fork stalling. *EMBO J* 25:5775–5782.
27. Colton SL, Xu XS, Wang YA, Wang G (2006) The involvement of ataxia-telangiectasia mutated protein activation in nucleotide excision repair-facilitated cell survival with cisplatin treatment. *J Biol Chem* 281:27117–27125.
28. Oakley GG *et al.* (2001) UV-induced hyperphosphorylation of replication protein A depends on DNA replication and expression of ATM protein. *Mol Biol Cell* 12:1199–1213.
29. Block WD, Yu Y, Lees-Miller SP (2004) Phosphatidyl inositol 3-kinase-like serine/threonine protein kinases (PIKKs) are required for DNA damage-induced phosphorylation of the 32 kDa subunit of replication protein A at threonine 21. *Nucleic Acids Res* 32:997–1005.
30. Zou Y, Liu Y, Wu X, Shell SM (2006) Functions of human replication protein A (RPA): From DNA replication to DNA damage and stress responses. *J Cell Physiol* 208:267–273.
31. Matsuoka S *et al.* (2007) ATM and ATR substrate analysis reveals extensive protein networks responsive to DNA damage. *Science* 316:1160–1166.
32. Wu X, Shell SM, Yang Z, Zou Y (2006) Phosphorylation of nucleotide excision repair factor xeroderma pigmentosum group A by ataxia telangiectasia mutated and Rad3-related-dependent checkpoint pathway promotes cell survival in response to UV irradiation. *Cancer Res* 66:2997–3005.
33. Wu X, Shell SM, Liu Y, Zou Y (2007) ATR-dependent checkpoint modulates XPA nuclear import in response to UV irradiation. *Oncogene* 26:757–764.
34. Gatei M *et al.* (2001) Ataxia telangiectasia mutated (ATM) kinase and ATM and Rad3 related kinase mediate phosphorylation of BRCA1 at distinct and overlapping sites. In vivo assessment using phospho-specific antibodies. *J Biol Chem* 276:17276–17280.
35. Hartman AR, Ford JM (2002) BRCA1 induces DNA damage recognition factors and enhances nucleotide excision repair. *Nat Genet* 32:180–184.
36. Chini CC, Chen J (2006) Repeated phosphopeptide motifs in human Claspin are phosphorylated by Chk1 and mediate Claspin function. *J Biol Chem* 281:33276–33282.
37. Praetorius-Ibba M *et al.* (2007) Role of Claspin in regulation of nucleotide excision repair factor DDB2. *DNA Repair* 6:578–587.
38. Olaussen KA *et al.* (2006) DNA repair by ERCC1 in non-small-cell lung cancer and cisplatin-based adjuvant chemotherapy. *N Engl J Med* 355:983–9891.
39. Bhana S, Hewer A, Phillips DH, Lloyd DR (2008) p53-dependent global nucleotide excision repair of cisplatin-induced intrastrand crosslinks in human cells. *Mutagenesis* 23:131–136.
40. O'Driscoll M *et al.* (2003) A splicing mutation affecting expression of ataxia-telangiectasia and Rad3-related protein (ATR) results in Seckel syndrome. *Nat Genet* 33:497–501.